

# Monocopper Doping in Cd-In-S Supertetrahedral Nanocluster via Two-Step Strategy and Enhanced Photoelectric Response

Tao Wu,<sup>\*,†,‡</sup> Qian Zhang,<sup>†</sup> Yang Hou,<sup>‡</sup> Le Wang,<sup>‡</sup> Chengyu Mao,<sup>‡</sup> Shou-Tian Zheng,<sup>§</sup> Xianhui Bu,<sup>§</sup> and Pingyun Feng<sup>\*,‡</sup>

<sup>†</sup>College of Chemistry, Chemical Engineering and Materials Science, Soochow University, Jiangsu 215123, China

<sup>‡</sup>Department of Chemistry, University of California, Riverside, California 92521, United States

<sup>§</sup>Department of Chemistry and Biochemistry, California State University, Long Beach, California 90840, United States

**S** Supporting Information

**ABSTRACT:** We apply a two-step strategy to realize ordered distribution of multiple components in one nanocluster (NC) with a crystallographically ordered core/shell structure. A coreless supertetrahedral chalcogenide Cd-In-S cluster is prepared, and then a copper ion is inserted at its void core site through a diffusion process to form a Cu-Cd-In-S quaternary NC. This intriguing molecular cluster with mono-copper core and Cd-In shell exhibits enhanced visible-light-responsive optical and photoelectric properties compared to the parent NC.

Doping and post-synthetic modification are important and effective tools in materials design and have been shown to promote the rapid development of practical materials, e.g., alloys,<sup>1</sup> metal oxides,<sup>2</sup> metal chalcogenides,<sup>3</sup> and even hybrid metal–organic frameworks,<sup>4</sup> by tuning their molecular and electronic structures to achieve some intriguing physical and chemical properties. In general, dopant atoms are prone to be randomly distributed in the host lattice. It is difficult to realize precise doping and accurate positioning of dopant atoms in 3D frameworks of dense or porous materials, especially in amorphous or polycrystalline form. A better understanding of doped structures will make it possible to establish structure/activity relationships for materials design from a theoretical perspective rather than trial-and-error experimental approaches.

There are several reasons for the increasing interest in the doping chemistry of nanosized cluster-based molecular compounds that could be characterized by single-crystal X-ray diffraction (SCXRD): (1) the distinct atomic environment (e.g., core, vertex, edge, and face sites) in a nanosized cluster induces site selectivity for dopant atoms; (2) the possibility of obtaining materials in high-quality crystal form facilitates precise probing of doping positions; (3) doped nanoclusters (NCs) could enhance or tune the intrinsic properties of the host frameworks or introduce novel properties. Some successful examples have been observed in transition-metal-ion-doped gold NCs,<sup>5</sup> endohedral metallic fullerene NCs,<sup>6</sup> and lanthanide-ion-doped Zintl NCs.<sup>7</sup> However, thus far, introducing specific dopants to desired positions at atomic scale to realize their ordered distribution remains a challenge in different NC systems. Toward this goal, new synthetic methods and strategies are needed.

We<sup>8</sup> and other research groups<sup>9</sup> have made significant advances in size and compositional tuning in nanoscale supertetrahedral chalcogenide clusters during the past decade. These clusters (denoted as T<sub>n</sub>, where *n* = number of metal sites along the edge of the tetrahedron), being structurally precise fragments of the well-known cubic ZnS-type semiconductors, can be regarded as the smallest semiconductor nanoparticles and exhibit size-dependent optical properties.<sup>10</sup> Unlike typical colloidal nanoparticles, these clusters can be analyzed via SCXRD, which could provide insight into various structure/property relationships. Recent studies on doping behavior in supertetrahedral clusters demonstrate that multiple factors affect the doping chemistry at different sites. For a T4-ZnGaSe cluster with 20 metal sites and 35 nonmetal sites, we successfully realized the site-selective and ordered distribution of two types of dopants (S and Sn) in a pentanary T4-ZnGaSnSeS cluster via synergistic effects of hard/soft acid/base theory and Pauling electrostatic valence sum rule.<sup>11</sup> The currently largest supertetrahedral cluster, T5 with 35 metal sites and 56 nonmetal sites (~2 nm in dimension), offers a unique opportunity to study the intriguing doping chemistry of NCs. So far, only the ternary (Cu/Cd/Zn)-(In/Ga)-S systems are known, and they exist either in an inter-connected pattern in 3D open frameworks<sup>12</sup> or in discrete molecular form with organic ligands as terminal groups in the crystal lattice.<sup>10,13</sup> Perhaps due to the relative difficulty in synthesizing discrete T5 clusters, no quaternary T5 cluster with compositionally ordered distribution has been known prior to this work. Our years of synthetic efforts have demonstrated that direct synthesis is ineffective in creating large quaternary T5 clusters with an ordered metal distribution.

Here we demonstrate a two-step strategy to realize ordered distribution of multiple components in a nanoscale supertetrahedral chalcogenide cluster with well-defined structure. A ternary molecular compound (denoted as ISC-10-CdInS, with ISC = isolated supertetrahedral cluster), composed of isolated coreless T5-CdInS clusters, is prepared for the first time, and subsequent diffusion of a single copper cation into its void core site forms a monocopper-doped quaternary ISC-10-CuCdInS phase (Figure 1). The presence of copper ion in the central site of the cluster is confirmed by SCXRD. The single copper ion in the T5-CuCdInS cluster dramatically changes the electronic

Received: April 26, 2013

Published: July 2, 2013

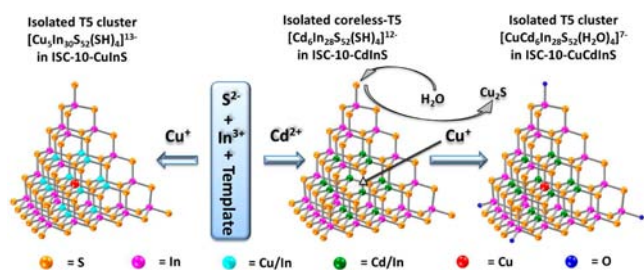


**Figure 1.** Two-step strategy for creating the quaternary T5-CuCdInS cluster with ordered site distribution; the templates are protonated organic molecules ( $\text{H}^+$ -DBN and  $\text{H}^+$ -PR).

structure of the parent cluster and allows it to exhibit an enhanced photoelectric response, especially in the visible-light region. Such precise doping behavior and an atomically ordered distribution rule are hard to imagine in doping chemistry of quaternary  $\text{Cu}_2\text{ZnSnS}_4$  colloidal nanocrystals similar in size to the T5 cluster.<sup>14</sup>

An octahedral crystal of ISC-10-CdInS was synthesized by solvothermal reaction of  $\text{Cd}(\text{NO}_3)_2$ , indium, and sulfur in the mixed solvents of 1,5-diazabicyclo[4.3.0]non-5-ene (DBN), piperidine (PR), and water at 190 °C for 12 days. Crystal structure refinement gave negatively charged isolated super-tetrahedral T5 clusters, packed together with organic counterions in the crystal lattice with  $I4_1/amd$  space group (Table S1). The resulting molecular formula was derived as  $[\text{H}^+-\text{DBN}]_8 \cdot [\text{H}^+-\text{PR}]_4 \cdot [\text{Cd}_6\text{In}_{28}\text{S}_{52}(\text{SH})_4]^{12-}$  by elemental analysis (Table S2) and structural refinement. Its phase purity was confirmed by powder XRD (PXRD; Figure S1).

The most prominent structural feature of ISC-10-CdInS is the isolated coreless T5 cluster with four  $-\text{SH}^-$  terminal groups and one core atom missing. In an ideal discrete T5 cluster, there is a tetrahedral  $\text{MS}_4$  core, and all other atoms are located on faces, edges, and corners. But in ISC-10-CdInS, the central metal atom bonded to four tetrahedrally coordinated  $\text{S}^{2-}$  sites is missing. T5 clusters without a core site were also reported by Li et al. ( $[\text{Cd}_6\text{In}_{28}\text{S}_{54}]^{12-}$ )<sup>9a</sup> and us ( $[\text{In}_{34}\text{S}_{54}]^{6-}$ );<sup>12a</sup> however, both types of clusters were part of 2D or 3D frameworks through corner-sharing, instead of existing in a discrete molecular form. The coreless cluster reported here is also different from our recently reported one, in which T5-CdInS cluster are capped by organic ligands serving as terminal group without the loss of its core site.<sup>10</sup>

The occurrence of a T5 cluster with or without a central metal site is determined by the specific reaction environment: (1) only one type of clusters exists in the solution which eventually gets crystallized or (2) two types of clusters with different negative charge coexist in solution. The cluster obtained in the final crystal could be mainly controlled by the reaction conditions (e.g., additional amount of core atom source, type of template molecules, and reaction temperature), which dictate the resulting crystallization process of various clusters. To better understand the factors affecting the occurrence of coreless T5-CdInS, we carried out a series of control experiments by systematically tuning the additional amount of Cd source while keeping other reactants unchanged (Table S3). Crystal structural refinement shows that crystals with the same structure are still obtained but their surfaces are coated with a tiny amount of hard-to-remove yellow CdS powder, identified through UV/vis absorption (Figure S2). Interestingly and unexpectedly, a new compound (denoted as OCF-43-CdInS, where OCF = organically

templated chalcogenide framework) is obtained when the amount of Cd source is >7-fold the original amount. OCF-43-CdInS has a 2D layer structure built from corner-sharing coreless T5-CdInS cluster layers (the same cluster as in ISC-10-CdInS) with the organic template molecules inserted between layers (Figure S3). The above control experiments suggest that the overall reaction condition, instead of the Cd amount, controls the coreless nature of the T5-CdInS cluster in ISC-10-CdInS.

Interestingly, the void core site in coreless T5-CdInS cluster could be expected to be filled with a third metal ion ( $\text{Cu}^+$  here) with smaller ionic radius than the two previously existing ones ( $\text{Cd}^{2+}$  and  $\text{In}^{3+}$ ). A new quaternary sample (denoted as ISC-10-CuCdInS) was prepared through a relatively mild solvothermal reaction of ground ISC-10-CdInS powder with CuCN and KCN in the mixed solvents (DBN, PR, and  $\text{H}_2\text{O}$ ) at 150 °C for 5 days (Table S4). Brown crystals with an original octahedral shape and smooth surface were obtained and identified to contain isolated T5-CuCdInS cluster, with the formula  $[\text{H}^+-\text{DBN}/\text{DBN}]_6 \cdot [\text{H}^+-\text{PR}/\text{PR}]_5 \cdot [\text{CuCd}_6\text{In}_{28}\text{S}_{52}(\text{H}_2\text{O})_4]^{7-}$  based on elemental analysis and structural refinement (Table S2, Figure S4). The central core site in this new discrete cluster is unmistakably filled with one copper ion, and the four corner sites are occupied by four water molecules instead of  $-\text{SH}^-$  groups. It is likely that  $-\text{SH}^-$  is replaced by  $\text{H}_2\text{O}$  because the  $-\text{SH}^-$  group has a higher reactivity, relative to other S sites in the cluster, which makes them easier removed, e.g., by formation of  $\text{Cu}_2\text{S}$ . In addition, replacement of  $-\text{SH}^-$  with  $\text{H}_2\text{O}$  can reduce the charge on the cluster, which could further stabilize the cluster.

To study the feasibility and rationality of diffusion of a copper ion into the core site from a structural perspective, a detailed comparison of the structural data around the tetrahedral  $\text{MS}_4$  core for the reported T5 clusters is carried out. As summarized in Table S5, the average distance between the central position and four adjacent  $\text{S}^{2-}$  sites in all coreless T5 clusters is  $\sim 2.22$  Å, much shorter than the Cd–S bond length in ISC-9-CdInS (2.37 Å).<sup>10</sup> When this site is partially occupied by  $\text{Cu}^+$ , with a site occupancy of 0.4, the distance increases slightly to 2.25 Å, and reaches up to 2.30 Å for the fully occupied case, which is very close to the corresponding Cu–S bond length (2.31 Å) in other T5-CuInS clusters. This comparison shows that the void space in the preformed coreless T5 cluster in ISC-10-CdInS is too small to hold one  $\text{Cd}^{2+}$  ion but could “breathe” to hold one  $\text{Cu}^+$  ion, which has a relatively smaller ionic radius than  $\text{Cd}^{2+}$ .

The diffusion of a single copper cation into the core of T5 clusters cannot be monitored *in situ* with our available techniques because of the use of a hydrothermal method that occurs in a “black box”. The primary thermodynamic driving force for copper ion diffusion could be charge reduction, which is regarded as a key point in stabilizing large clusters with highly negative charge. The charge of the T5-CdInS cluster in ISC-10-CdInS was drastically reduced by 5 when the cluster was transformed into T5-CuCdInS with four negatively charged  $-\text{SH}^-$  replaced by neutral water molecules and the core site filled with one positive charge.

The discrete form of the coreless T5 cluster plays a crucial role in allowing copper diffusion to proceed and be characterized by SCXRD, which leads to the precise doping behavior. Previously, we envisioned that the two aforementioned compounds<sup>9a,12a</sup> with coreless T5 clusters were good candidates to undergo the two-step strategy for embedding one small-sized metal ion (here  $\text{Cu}^+$ ) into its core site, yet that strategy was unsuccessful. One possible reason is that T5 clusters in 2D or 3D rigid frameworks are less likely to be exposed to the copper ions to permit

complete diffusion of freely moving metal cations in the whole micrometer-sized crystals. In addition, forming or maintaining high-quality crystals during the doping process under solvothermal treatment is more problematic for 2D or 3D covalent crystals. For 2D and 3D frameworks, poor crystallinity makes it difficult to determine the precise doping site through the SCXRD technique, although copper ions in the resulting products could be identified through elemental analysis and the sample color change from pale yellow to brown. Unlike the above two compounds, ISC-10-CdInS shows certain solubility in reaction solution due to its molecular nature, as confirmed by two recrystallization processes where the ground fine powder could recover its octahedral-shaped crystal after solvothermal treatment in fresh reaction solvent and the Cu-doped T5 clusters display a different packing pattern in ISC-10-CuCdInS since the cell parameters are distinct from those of its parent crystals. Clearly, the intrinsic solubility and dispersibility of the isolated coreless T5 cluster facilitate the copper-diffusion-based doping process.

To better understand the effects of copper doping on the properties of ISC-10-CdInS and ISC-10-CuCdInS, we also prepared ISC-10-CuInS pure phase without a Cd component under reaction conditions similar to those used for ISC-10-CdInS. This formed brown crystals also feature a discrete T5 cluster with the formula of  $[\text{H}^+-\text{DBN}]_7 \cdot [\text{H}^+-\text{PR}]_6 \cdot [\text{Cu}_3\text{In}_{30}\text{S}_{52}(\text{SH})_4]^{13-}$  as evidenced by PXRD and elemental analysis. Even though no good-quality crystals were obtained for determination of its core site through structural refinement, the ratio of Cu:In (5:30) was in good agreement with the typical T5-CuInS cluster, indicating that the core site is loaded with copper ion instead of being empty.

Solid-state diffuse reflectance UV/vis spectra were studied by using crystalline samples of ISC-10's. In general, Cu-containing In-S systems exhibit a red-shifted absorption band compared to that of the parent frameworks.<sup>15</sup> This is also observed in the current case. From the absorption edges (Figure 2), the band gaps as determined using Kubelka–Munk methods are 3.01 eV for ISC-10-CdInS, 2.11 eV for ISC-10-CuCdInS, and 2.29 eV for ISC-10-CuInS. The results indicate that the three cluster-based molecular compounds have band absorption behavior similar to that observed in 2D or 3D extended solid semiconductor materials of similar chemical compositions. Notably, ISC-10-CdInS exhibits band gaps similar to those of OCF-43-CdInS (3.01 eV) and Li's cluster (3.00 eV),<sup>9a</sup> both of which have extended 2D frameworks with the same coreless T5-CdInS cluster. These results show that the nature of the cluster plays a

more dominant role in the optical property than their connectivity modes in the solid structure of the materials. This is further supported by the data for the T5-CuInS cluster. The band gap of ISC-10-CuInS is comparable with that of the reported molecular compound (2.28 eV)<sup>13</sup> and its extended framework (2.20 eV)<sup>16</sup> based on the T5-CuInS cluster. All of them exhibit blue-shifts compared with the band gap of bulk  $\text{CuInS}_2$  (1.53 eV), which has an elemental composition and metal ion coordination environment similar to those found in the T5-CuInS NC.<sup>17</sup> The precise copper doping in the T5-CuCdInS cluster significantly altered the electronic structure and optical property and made its absorption edge much lower than that of a T5-CdInS cluster without copper, even lower than that of a T5-CuInS cluster with more copper ions.

To further investigate the semiconducting property of these cluster-based molecular compounds, we studied the visible-light-driven photoelectric response of ISC-10 materials. We fabricated photoanodes by using direct current electrophoretic deposition (ED) to modify a F-doped  $\text{SnO}_2$  (FTO) electrode with a thin layer of ground ISC-10 samples, which were pre-dispersed in isopropanol with a small amount of  $\text{Mg}(\text{NO}_3)_2$  electrolytes. These modified electrodes have similar thickness ( $\sim 10 \mu\text{m}$ ) and morphology and retain their original frameworks of film materials during the process of ED, as characterized and confirmed by PXRD and EDS (Figures S1 and S5). A standard three-electrode system was then applied to detect the transient photocurrent density of the above three modified electrodes under visible-light irradiation (wavelength  $> 420 \text{ nm}$ ). (See SI for details of preparation and measurement, Scheme S1.) The photocurrent traces in Figure 3 show a rapid response and good reproducibility for all ISC-10 electrodes at the start and end of illumination. The photocurrent density of the ISC-10-CuCdInS electrode is almost 10-fold that of ISC-10-CdInS and half that of ISC-10-CuInS. Higher photocurrent density indicates better generation and separation of photoinduced electron/hole pairs in FTO electrodes with Cu-doped samples; furthermore, only a small amount of dopant atom led to significant differences. We also measured the current–voltage curves of ISC-10's in the dark and under visible-light illumination (Figure S6). All electrodes show negligible current under dark conditions. Upon irradiation, both ISC-10-CuCdInS and ISC-10-CuInS show higher photocurrent and much more rapid increase compared with ISC-10-CdInS. The appearance of the anodic photocurrent suggests that ISC-10's are typical n-type semiconductor materials.<sup>18</sup>

In addition to charge separation, the charge-transfer capability of photoelectrodes with different ISC-10's could also be affected by the presence of copper ions in T5 clusters. We conducted alternating current impedance experiments to study differences in the electron transport behavior. The enhanced electrical conductivity of electrodes with Cu-doped materials is confirmed by electrochemical impedance spectroscopy (EIS) at low frequencies. Figure 3b shows Nyquist plots. It is known that the radius of each arc in a Nyquist plot is associated with the charge-transfer process at the corresponding electrode, and a smaller radius is correlated with a lower charge-transfer resistance.<sup>19</sup> A reduced charge-transfer resistance under irradiation was found for all the studied photoelectrodes because the arc radius under irradiation is consistently smaller than that in the dark (Figure S7). This could be attributed to the improved current density as a result of the rich photogenerated electron/hole pairs on the electrodes. The ISC-10-CuCdInS electrode shows a much smaller radius of the semicircle than does the ISC-10-CdInS electrode both in the dark and under irradiation. By

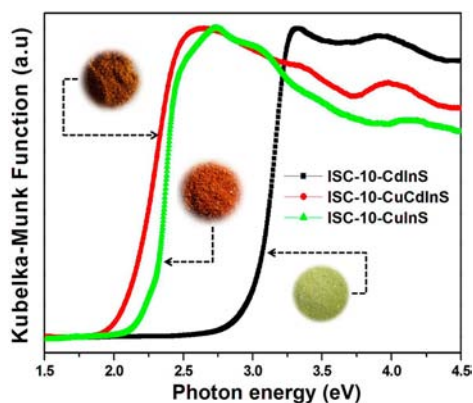
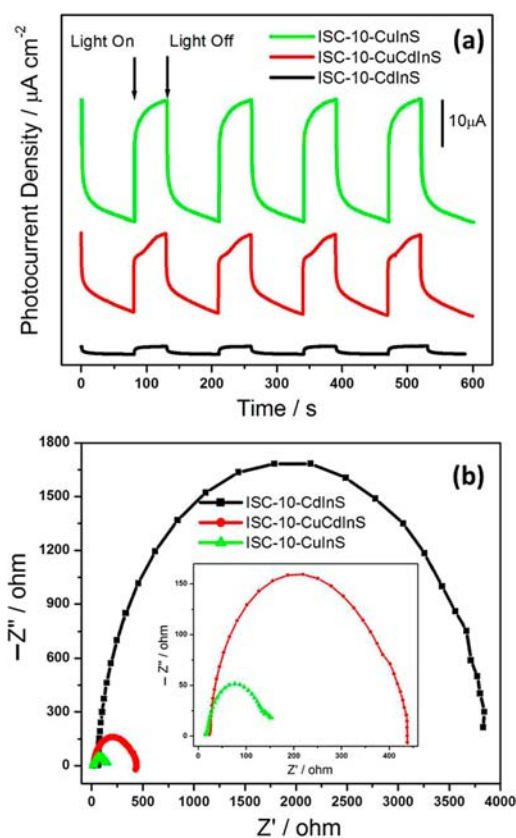


Figure 2. Normalized solid-state diffuse reflectance spectra of ISC-10's.





**Figure 3.** (a) Transient photocurrent density versus time plotted for the electrodes functionalized with the ground materials of ISC-10's. (b) Nyquist plots of the three electrodes (inset, enlarged plot).

fitting EIS to a simulated model of the simple equivalent circuits (as shown in Table S6), we find that the charge-transfer resistance in ISC-10-CuCdInS electrode is much lower than in ISC-10-CdInS electrode (400.9 vs 3732  $\Omega$ ), indicating an effective transfer of photogenerated electron/hole pairs at electrodes with Cu-doped samples. The increased photocurrent density could likewise account for the ameliorative electrical conductivity behavior. Higher electrical conductivity was also observed on the ISC-10-CuInS electrode (133.1  $\Omega$ ) with more copper content; however, it exhibits only a slight improvement compared to the ISC-10-CuCdInS electrode. Although the solid samples of ISC-10's are not good conducting materials, their electrical conductivity values show a similar trend as observed above (Table S7). From these results, it is clear that precise doping of one copper ion at a specific position (the core site in this case) in the supertetrahedral-cluster-based molecule compound may cause a big difference in its photoelectric response performance.

In conclusion, we have successfully realized the first ordered distribution of multiple components in one nanoscale supertetrahedral chalcogenide cluster with a well-defined structure through a two-step synthetic strategy. A single transition-metal cation,  $\text{Cu}^+$ , is shown to be capable of diffusing into the core site of an isolated coreless T5 cluster. The precise doping behavior and accurate positioning prompted us to probe the electronic structure and optical properties of these compositionally tunable semiconducting clusters. This study highlights the possibility of cation diffusion for accessing the center of a nanosized cluster with hollow structure at the atomic scale, and it presents a special

route toward the fine modification of photoelectrical properties of semiconductor materials.

## ■ ASSOCIATED CONTENT

### Supporting Information

Experimental conditions, elemental analysis, additional structures, PXRD data, and SEM and optical images. This material is available free of charge via the Internet at <http://pubs.acs.org>.

## ■ AUTHOR INFORMATION

### Corresponding Author

wutao@suda.edu.cn; pingyun.feng@ucr.edu

### Notes

The authors declare no competing financial interest.

## ■ ACKNOWLEDGMENTS

We thank NSF (P.F., DMR-1200451), NSFC (T.W., NSFC-21271135), and a start-up fund (T.W., Q410900712) from Soochow University for support of this work.

## ■ REFERENCES

- (1) Vinayan, B. P.; Nagar, R.; Rajalakshmi, N.; Ramaprabhu, S. *Adv. Funct. Mater.* **2012**, *22*, 3519.
- (2) Zhang, S.; Saito, T.; Mizumaki, M.; Chen, W.-T.; Tohyama, T.; Shimakawa, Y. *J. Am. Chem. Soc.* **2013**, *135*, 6056.
- (3) Manos, M. J.; Kanatzidis, M. G. *J. Am. Chem. Soc.* **2009**, *131*, 6599.
- (4) Yang, H.; He, X.-W.; Wang, F.; Kang, Y.; Zhang, J. *J. Mater. Chem.* **2012**, *22*, 21849.
- (5) Qian, H.; Jiang, D.-e.; Li, G.; Gayathri, C.; Das, A.; Gil, R. R.; Jin, R. *J. Am. Chem. Soc.* **2012**, *134*, 16159.
- (6) Yamada, M.; Akasaka, T.; Nagase, S. *Acc. Chem. Res.* **2009**, *43*, 92.
- (7) (a) Lips, F.; Clérac, R.; Dehnen, S. *Angew. Chem., Int. Ed.* **2011**, *50*, 960. (b) Lips, F.; Holyńska, M.; Clérac, R.; Linne, U.; Schellenberg, I.; Pöttgen, R.; Weigend, F.; Dehnen, S. *J. Am. Chem. Soc.* **2012**, *134*, 1181.
- (8) (a) Zheng, N.; Bu, X.; Wang, B.; Feng, P. *Science* **2002**, *298*, 2366. (b) Zheng, N.; Bu, X.; Feng, P. *Nature* **2003**, *426*, 428. (c) Feng, P.; Bu, X.; Zheng, N. *Acc. Chem. Res.* **2005**, *38*, 293.
- (9) (a) Su, W. P.; Huang, X. Y.; Li, J.; Fu, H. X. *J. Am. Chem. Soc.* **2002**, *124*, 12944. (b) Li, H.; Laine, A.; O'Keefe, M.; Yaghi, O. M. *Science* **1999**, *283*, 1145. (c) Wang, Y.-H.; Zhang, M.-H.; Yan, Y.-M.; Bian, G.-Q.; Zhu, Q.-Y.; Dai, J. *Inorg. Chem.* **2010**, *49*, 9731. (d) Palchik, O.; Lyer, R. G.; Liao, J. H.; Kanatzidis, M. G. *Inorg. Chem.* **2003**, *42*, 5052. (e) Zimmermann, C.; Anson, C. E.; Weigend, F.; Clérac, R.; Dehnen, S. *Inorg. Chem.* **2005**, *44*, 5686. (f) Brandmayer, M. K.; Clérac, R.; Weigend, F.; Dehnen, S. *Chem.—Eur. J.* **2004**, *10*, 5147.
- (10) Wu, T.; Bu, X.; Liao, P.; Wang, L.; Zheng, S.; Ma, R.; Feng, P. *J. Am. Chem. Soc.* **2012**, *134*, 3619.
- (11) Wu, T.; Bu, X.; Zhao, X.; Khazhaky, R.; Feng, P. *J. Am. Chem. Soc.* **2011**, *133*, 9616.
- (12) (a) Wang, C.; Bu, X.; Zheng, N.; Feng, P. *J. Am. Chem. Soc.* **2002**, *124*, 10268. (b) Bu, X.; Zheng, N.; Li, Y.; Feng, P. *J. Am. Chem. Soc.* **2002**, *124*, 12646.
- (13) Xiong, W.-W.; Li, J.-R.; Hu, B.; Tan, B.; Li, R.-F.; Huang, X.-Y. *Chem. Sci.* **2012**, *3*, 1200.
- (14) (a) Steinhagen, C.; Panthani, M. G.; Akhavan, V.; Goodfellow, B.; Koo, B.; Korgel, B. A. *J. Am. Chem. Soc.* **2009**, *131*, 12554. (b) Guo, Q.; Hillhouse, H. W.; Agrawal, R. *J. Am. Chem. Soc.* **2009**, *131*, 11672.
- (15) Wang, X.; Pan, D.; Weng, D.; Low, C.-Y.; Rice, L.; Han, J.; Lu, Y. *J. Phys. Chem. C* **2010**, *114*, 17293.
- (16) Wang, L.; Wu, T.; Zuo, F.; Zhao, X.; Bu, X.; Wu, J.; Feng, P. *J. Am. Chem. Soc.* **2010**, *132*, 3283.
- (17) Tell, B.; Shay, J. L.; Kasper, H. M. *Phys. Rev. B* **1971**, *4*, 2463.
- (18) Zhang, Q.; Liu, Y.; Bu, X.; Wu, T.; Feng, P. *Angew. Chem., Int. Ed.* **2008**, *47*, 113.
- (19) Bell, N. J.; Ng, Y. H.; Du, A.; Coster, H.; Smith, S. C.; Amal, R. *J. Phys. Chem. C* **2011**, *115*, 6004.